Experimental confirmation of spin gap in antiferromagnetic alternating spin-3/2 chain substances $R\mathrm{CrGeO_5}$ (R = Y or ^{154}Sm) by inelastic neutron scattering experiments

Masashi Hase[1],* Minoru Soda[2], Takatsugu Masuda[2], Daichi Kawana[2,3], Tetsuya Yokoo[3], Shinichi Itoh[3], Akira Matsuo[2], Koichi Kindo[2], and Masanori Kohno[1]

[1]*National Institute for Materials Science (NIMS), Tsukuba, Ibaraki 305-0047, Japan*

[2] *The Institute for Solid State Physics (ISSP), the University of Tokyo, Kashiwa, Chiba 277-8581, Japan*

[3]*High Energy Accelerator Research Organization (KEK), Tsukuba, Ibaraki 305-0801, Japan*

(Dated: April 28, 2014)

arXiv:1404.6297v1 [cond-mat.str-el] 25 Apr 2014

Abstract

A spin-singlet ground state with a spin gap has been discovered in antiferromagnetic spin chain substances when the spin value is 1/2, 1 or 2. To find spin gap (singlet-triplet) excitations in spin-3/2 chain substances, we performed inelastic neutron scattering and magnetization measurements on $R\mathrm{CrGeO_5}$ (R = Y or Sm) powders. As expected, we observed spin gap excitations and the dispersion relation of the lowest magnetic excitations. We proved that the spin system of Cr^{3+} was an antiferromagnetic alternating spin-3/2 chain.

PACS numbers: 75.10.Pq, 75.10.Kt, 75.40.Gb

*Electronic address: HASE.Masashi@nims.go.jp

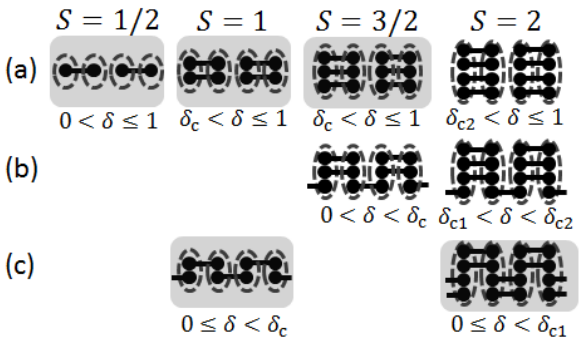

FIG. 1: (Color online) The valence-bond-solid (VBS) diagrams.[3] The spin-singlet ground state shown in (a), (b), and (c) is designated $(2S, 0)$, $(2S-1, 1)$, and (S, S) states, respectively. Small circles and lines represent spin-1/2 variables and singlet pairs, respectively. Each ellipse represents the symmetrization of the spin-1/2 variables on each site to create the total spin variable. The ground states are accompanied with a spin gap. The value of δ of gapless points is 0 for $S = 1/2$, $\delta_c = 0.2595(5)$ for $S = 1$,[2] 0 and $\delta_c = 0.42(2)$ for $S = 3/2$,[3] and $\delta_{c1} = 0.18(1)$ and $\delta_{c2} = 0.545(5)$ for $S = 2$.[4] Model substances were found for the hatched GSs when $S = 1/2, 1$, and 2, as described in the text. In this study, we show that RCrGeO$_5$ (R = Y or Sm) are model substances for the hatched GS of $S = 3/2$ (a).

I. INTRODUCTION

The ground state (GS) is spin singlet in antiferromagnetic (AF) Heisenberg alternating spin chains because of large quantum fluctuation. The Hamiltonian is given as follows.

$$\mathcal{H} = J \sum_i [1 - (-1)^i \delta] \boldsymbol{S}_i \cdot \boldsymbol{S}_{i+1}. \tag{1}$$

In the AF Heisenberg uniform ($\delta = 0$) spin-1/2 chain, GS is almost an ordered state in spite of spin singlet (critical state) and is designated the gapless Tomonaga-Luttinger liquid (TLL). A gapless GS can also appear when the spin value S is larger than 1/2.[1–4] The gapless GS is regarded as TLL. A spin gap (singlet-triplet gap) opens except for gapless point(s) and a spin-singlet GS is stabilized. The spin-singlet GS can be expressed using valence-bond-solid (VBS) diagrams, as depicted in Fig. 1.[3] Considering the range of δ in which VBS exists, the appearance of the spin gap is a common phenomenon in AF alternating spin chains.

Model substances have been found for the hatched GSs in Fig. 1 when $S = 1/2, 1$, and 2. Cu(NO$_3$)$_2$-2.5H$_2$O,[5, 6] TTF-MS$_4$C$_4$(CF$_3$)$_4$ (M= Cu or Au, TTF=tetrathiafulvalene),[7,

8] and $CuGeO_3$[9–11] are model substances for $S = 1/2$ (a). [Ni(*N, N'*-bis(3-aminopropyl)propane-1, 3-diamine(μ-NO_2)]ClO_4 (abbreviated as NTENP).[12, 13] is a model substance for $S = 1$ (a). $Ni(C_2H_8N_2)_2NO_2(ClO_4)$ (abbreviated as NENP)[14] and Y_2BaNiO_5[15–17] are model substances for $S = 1$ (c).

When the spin value is larger than 1, almost no model substance exists. The only example reported in the literature is $MnCl_3(C_{10}H_8N_2)$.[18] This substance has an AF uniform spin-2 chain of which GS is shown by the diagram of $S = 2$ (c). The energy gap was evaluated as 0.32(8) meV and 0.14(3) meV from magnetization curves at 30 mK in the magnetic field parallel and perpendicular to chains, respectively. These gaps are consistent with a Haldane gap of 0.20(7) meV, where the excited triplet is split by single-ion anisotropy $D = 0.03(1)$ meV. The temperature T dependence of magnetic susceptibility and the magnetization curve were well fitted to calculated results with $J = 31.2$ K and the g-value of 2.02.[19] Inelastic neutron scattering results provide microscopic evidence for the presence of the Haldane gap.[20]

We comment on AF Heisenberg uniform spin chain substances AMX_3. Here, A is K, Rb or Cs, M is $3d$ atom, and X is F, Cl or Br. In the uniform spin-1 chain substance $CsNiCl_3$, the Haldane gap was observed in inelastic neutron scattering experiments.[21] In the uniform spin-3/2 chain substances $CsVCl_3$ and $CsVBr_3$, low-energy broad excitations were observed at the magnetic zone center at 20 K ($> T_N = 13.3$ K)[22] and 25 K ($> T_N = 20.3$ K),[23] respectively, where T_N is an AF transition temperature. The low-energy broad excitations were recognized as a part of the continuum just above the lowest magnetic excitations. Therefore, the experimental results do not contradict the theoretical prediction (gapless excitations). In the uniform spin-2 chain substance $CsCrCl_3$, no excitation gap was detected at the magnetic zone center at 20 K ($> T_N = 16$ K) within the experimental errors.[24] The Haldane gap can be estimated to be 0.2 meV and is predicted to be observable below 1.4 K. Thus, the Haldane gap were unable to be detected in the experiments.

We can show experimentally that the appearance of the spin gap is a universal phenomenon irrespective of the spin value below 2 if we can find the spin gap in an AF alternating spin-3/2 chain substance. We have devoted attention to insulating RCrGeO$_5$ (R = Y or rare earth) as shown in Fig. 2.[25] A Cr^{3+} ion is surrounded by O^{2-} ligands and forms a CrO_6 octahedron. In the ground state of Cr^{3+} ions, the orbital degree of freedom is quenched. Spin 3/2 is responsible for the magnetism of Cr^{3+} ions. From the crystal

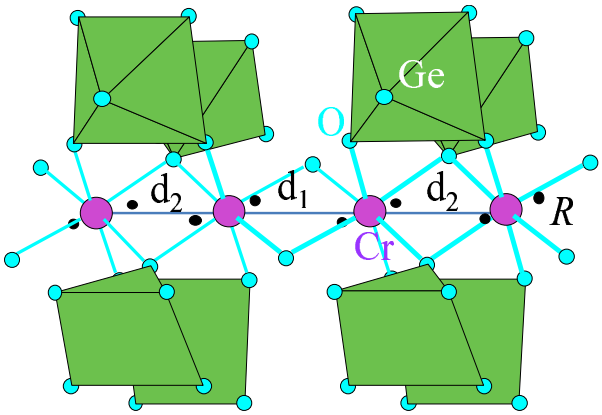

FIG. 2: (Color online) A part of the RCrGeO$_5$ structure showing two kinds of Cr-Cr bonds in the chain of edge-sharing CrO$_6$ octahedra, GeO$_5$ square pyramids, and R atoms.

structure, Cr^{3+} spins are expected to form an alternating spin-3/2 chain. Table I shows the Cr-O-Cr angle and Cr-Cr distance in two kinds of Cr-Cr bonds (d_1 and d_2 bonds). Spin chains are separated from one another by GeO$_5$ square pyramids and R^{3+} ions. Shpanchenko *et al.* reported the T dependence of magnetic susceptibility (χ) of RCrGeO$_5$ (R = Sm, Eu or Nd) powders.[25] A broad maximum of χ appears at $T_{\rm max}$ = 220 K and 100 K in SmCrGeO$_5$ and EuCrGeO$_5$, respectively, indicating the existence of a low-dimensional AF spin system. Considering the crystal structure and the large values of $T_{\rm max}$, we can expect that Cr^{3+} spins form an AF Heisenberg alternating spin-3/2 chain. No magnetic transition appears down to 1.8 K in the two substances. In NdCrGeO$_5$, χ of Nd^{3+} ions is very large. We cannot determine whether χ of Cr^{3+} spins shows a broad maximum or not. Probably, an AF alternating spin-3/2 chain also exists in NdCrGeO$_5$ because of the same crystal structure. A clear peak appears at 2.6 K in χ of NdCrGeO$_5$. The susceptibility of Nd^{3+} ions is dominant at low T. Probably, Nd^{3+} magnetic moments generate a magnetic transition.

As T is lowered, the susceptibility of RCrGeO$_5$ (R = Sm, Eu or Nd) increases like a Curie-Weiss susceptibility. The increase originates in rare earth ions or magnetic other materials. The susceptibility becomes nearly zero at low T if a spin-singlet ground state with a spin gap exists in the Cr^{3+} spin system. Because of the Curie-Weiss susceptibility at low T, unfortunately, we cannot prove a spin-singlet ground state with a spin gap from the susceptibility results. Consequently, we performed inelastic neutron scattering (INS) and magnetization measurements on RCrGeO$_5$ (R = Y or Sm) powders to confirm the spin gap

TABLE I: Cr-O-Cr angles and Cr-Cr distances in two kinds of Cr-Cr bonds (d_1 and d_2 bonds) in RCrGeO$_5$ (R = Y or Sm).[25]

		Y	Sm
d_1 bond	Cr-O-Cr angle	95.9°	97.3°
	Cr-Cr distance	2.872 Å	2.952 Å
d_2 bond	Cr-O-Cr angle	92.8°	91.3°
	Cr-Cr distance	2.811 Å	2.770 Å

(singlet-triplet) excitations.

II. METHODS OF EXPERIMENTS AND CALCULATIONS

Crystalline powders of RCrGeO$_5$ (R = Y or Sm) were synthesized using a solid-state-reaction method at 1,523 K in air with intermediate grindings.[25] We used an isotope ^{154}Sm (purity of the isotope: 99 %) for powders of INS experiments to decrease absorption of neutrons. We confirmed formation of RCrGeO$_5$ (R = Y or Sm) using an X-ray diffractometer (RINT-TTR III; Rigaku). We were able to obtain samples of a nearly single phase of SmCrGeO$_5$. We found the existence of non-magnetic $Y_2Ge_2O_7$ in diffraction patterns of YCrGeO$_5$ samples. The molar ratio of $Y_2Ge_2O_7$ was estimated roughly as 10 % from diffraction intensities.

We measured magnetizations up to H = 5 T using a superconducting quantum interference device (SQUID) magnetometer (MPMS-5S; Quantum Design). High-field magnetization measurements were conducted using an induction method with a multilayer pulsed field magnet installed at the Institute for Solid State Physics (ISSP), the University of Tokyo. We performed inelastic neutron scattering measurements using the High Resolution Chopper (HRC) spectrometer at BL 12 in Japan Proton Accelerator Research Complex (J-PARC).[26–28] The energy resolution at the energy transfer ω = 0 meV is 3 - 5 % of $E_{\rm i}$ (the energy of incident neutrons). The Q resolution is better than 0.1 Å^{-1} where Q is the magnitude of the scattering vector.

We calculated susceptibility of AF Heisenberg alternating spin-3/2 chains [Eq. (1)] using the quantum Monte Carlo loop algorithm[29] on 240 site chains. Finite-size effects and

statistical errors are negligible in the scales of figures represented in this paper. We calculated the dynamical structure factor, which is proportional to neutron scattering intensity, on 120 site chains under the open boundary condition using the dynamical density-matrix renormalization group (DMRG) method.[30]

III. RESULTS AND DISCUSSION

We show χ of $YCrGeO_5$ and $SmCrGeO_5$ powders as red circles in Figs. 3(a) and 3(b), respectively. The value of the applied magnetic field is 0.01 T. The molar ratio of $Y_2Ge_2O_7$ included in the $YCrGeO_5$ sample was estimated as 8.8 %. Considering the $Y_2Ge_2O_7$ weight, we obtained the susceptibility in Fig. 3(a). The susceptibility of $YCrGeO_5$ at low T increases like a Curie-Weiss susceptibility probably because of unidentified magnetic material(s) in the $YCrGeO_5$ sample. We were unable to prove a spin-singlet ground state with a spin gap because of the Curie-Weiss susceptibility. No magnetic transition appears down to 2 K. The susceptibility of our $SmCrGeO_5$ powders agrees with that reported by Shpanchenko *et al.*[25] Results of analyses are described later.

We show high-field magnetizations at 4.2 K of $YCrGeO_5$ and $SmCrGeO_5$ powders in Figs. 4(a) and 4(b), respectively. An upturn of the magnetization of $YCrGeO_5$ is apparent around 55 T, suggesting spin-gap closing induced by the magnetic field. The spin-gap closing might occur in higher fields. The slope of the magnetization is small around $M = 0.15\ \mu_B$/formula unit, indicating that about 5 % Cr^{3+} spins are nearly isolated. We did not observe an upturn in the magnetization of $SmCrGeO_5$ up to 58 T. The magnetization results suggest that $YCrGeO_5$ has a smaller spin gap than $SmCrGeO_5$. This point is consistent with INS results presented below.

We show INS results of $YCrGeO_5$ at 4.0 K and 199 K in Figs. 5(a) and 5(b), respectively, and those of $^{154}SmCrGeO_5$ at 7.8 K and 202 K in Figs. 6(a) and 6(b), respectively. The energies of incident neutrons E_i are 51.1 and 91.6 meV for the measurements of $YCrGeO_5$ and $^{154}SmCrGeO_5$, respectively. In $YCrGeO_5$, excitations are observed in the energy range of 8 meV $\lesssim \omega \lesssim$ 23 meV at 4.0 K and the intensity decreases with the increase of Q. The intensity of the excitations is suppressed at higher temperature, 199 K. The results mean that the observed excitations are dominated by those of magnetic origin. Furthermore no excitation is observed at $\omega \lesssim 8$ meV and this means the existence of spin gap. Qualitatively

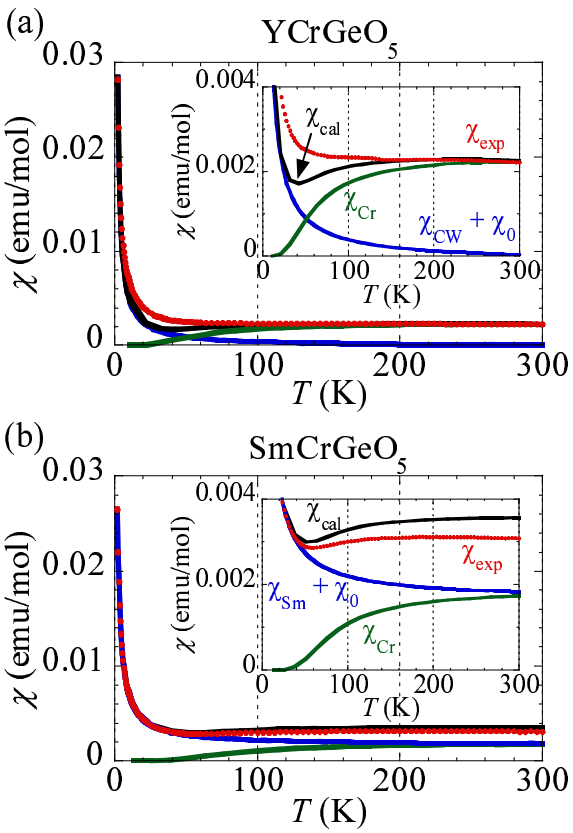

FIG. 3: (Color online) Magnetic susceptibility in 0.01 T of $YCrGeO_5$ (a) and $SmCrGeO_5$ (b). The insets represent χ below 0.004 emu/mol. Circles show the experimental results. Three lines in each figure are explained in the text.

the same behaviors are observed in $^{154}SmCrGeO_5$. $YCrGeO_5$ and $^{154}SmCrGeO_5$ are the first spin-3/2 chain substances having a spin gap.

We obtained intensity maps in the $k-\omega$ plane as shown in Figs. 7(a) and 8(a) from the low T data using the conversion method developed by Tomiyasu *et al.*[31] The formula is given as follows.

$$S^{(1D)}_{SX}(Q_{1D},\omega) = [S_{pwd}(Q,\omega) + Q\frac{\partial S_{pwd}(Q,\omega)}{\partial Q}]_{Q=Q_{1D}}. \quad (2)$$

Here, Q_{1D}, $S_{pwd}(Q,\omega)$, and $S^{(1D)}_{SX}(Q_{1D},\omega)$ represent the magnitude of the scattering vector parallel to the spin chain, the powder average scattering function, and the scattering function for Q_{1D} expected in a single crystal, respectively. The normalized wavenumber k is defined as $Q_{1D}\frac{d_1+d_2}{2}$. The values of d_1+d_2 at room temperature are 5.68 and 5.72 Å for $YCrGeO_5$

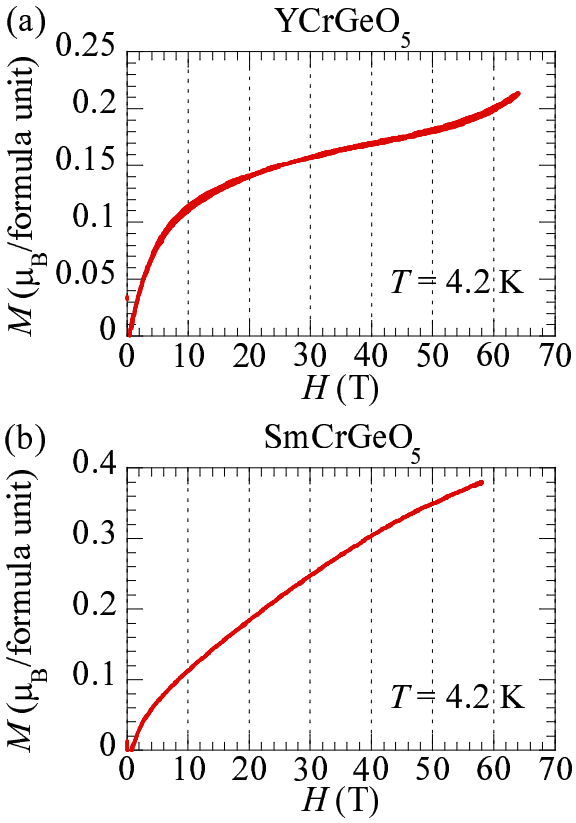

FIG. 4: (Color online) High-field magnetization at 4.2 K of $YCrGeO_5$ (a) and $SmCrGeO_5$ (b).

and $SmCrGeO_5$, respectively.[25] The intensity is the strongest at around $k = \pi$, as expected in AF alternating spin chains. The magnetic excitations seem to have a dispersion relation. The white line in Figs. 7(a) and 8(a) shows the empirical dispersion relation of the lowest magnetic excitations $\omega(k) = \sqrt{A^2 \sin^2 k + \Delta^2}$. The values are $\Delta = 10$ meV and $A = 20$ meV in $YCrGeO_5$, and $\Delta = 18$ meV and $A = 15$ meV in $^{154}SmCrGeO_5$.

We compare experimental INS intensities and calculated dynamical structure factors of the AF Heisenberg alternating spin-3/2 chains. The experimental values of $\omega(1.5\pi)/\omega(\pi)$ are 2.2 and 1.3 in $YCrGeO_5$ and $^{154}SmCrGeO_5$, respectively. When $\delta = 0.75$ and 0.90, values of $\omega(1.5\pi)/\omega(\pi)$ are 2.2 and 1.3 in the calculated results presented in Figs. 7(b) and 8(b), respectively. The calculated dynamical structure factors are similar to the experimental INS intensities. In the calculated result with $\delta = 0.75$, $\Delta/J = 1.1$. Therefore, $J = 9.1$ meV $= 106$ K in $YCrGeO_5$. The ratio of the two exchange interaction values is $(1-\delta)/(1+\delta) = 0.14$. In the calculated result with $\delta = 0.90$, $\Delta/J = 1.6$. Therefore, $J = 11$ meV $= 128$ K in

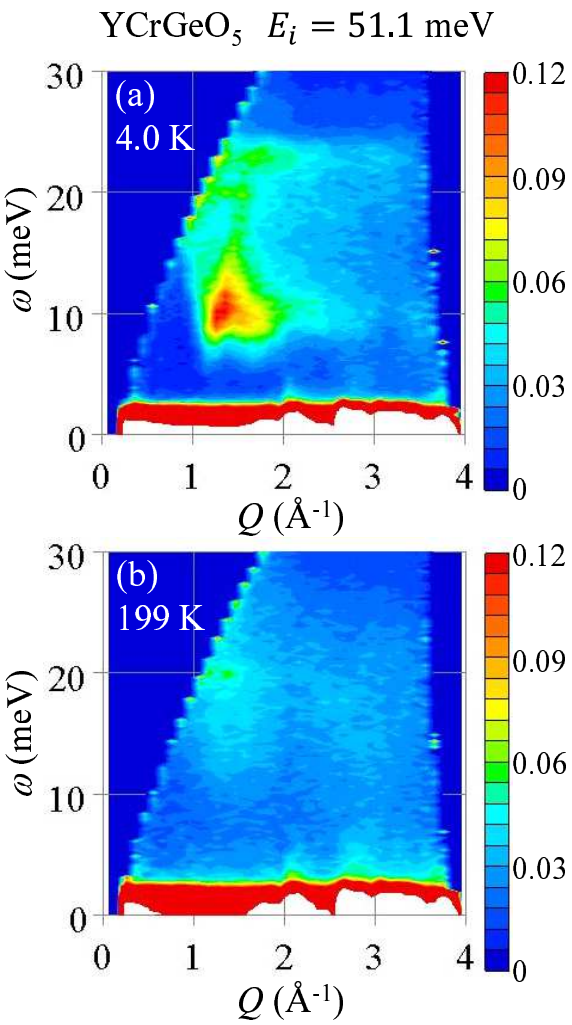

FIG. 5: (Color online) Maps of neutron scattering intensity in the $Q-\omega$ plane of $YCrGeO_5$ at 4.0 K (a) and 199 K (b). The energy of incident neutrons E_i is 51.1 meV. The numbers of protons injected to the neutron production target are about 1.47×10^{19} and 1.30×10^{19} for the measurements at 4.0 K and 199 K, respectively. When the beam power is 200 kW, the total number of protons per day is 3.6×10^{19}. The spent times are about 9.8 and 8.7 hr for the measurements at 4.0 K and 199 K, respectively. The right vertical keys show the INS intensity in arbitrary units. The intensity is normalized to compare two data in different proton numbers.

$^{154}SmCrGeO_5$. The value of $(1-\delta)/(1+\delta)$ is 0.05.

Figures 7(c) and 8(c) show constant Q spectra at $k = \pi$ of $YCrGeO_5$ at 4.0 K and $^{154}SmCrGeO_5$ at 7.8 K, respectively. A single peak is apparent around the gap energy in

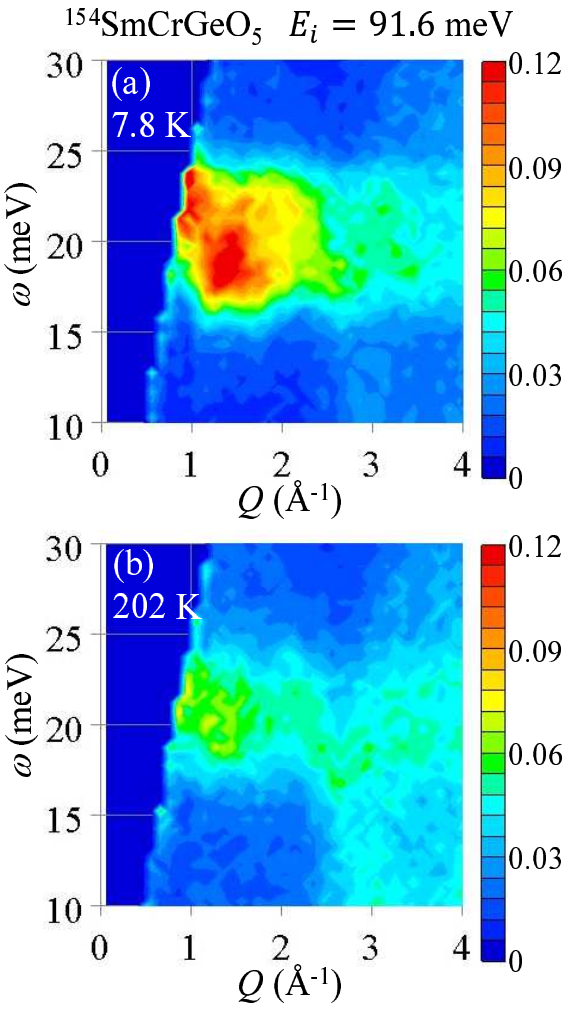

FIG. 6: (Color online) Maps of neutron scattering intensity in the $Q-\omega$ plane of ^{154}SmCrGeO$_5$ at 7.8 K (a) and 202 K (b). The energy of incident neutrons $E_{\rm i}$ is 91.6 meV. The numbers of protons injected to the neutron production target are about 2.79×10^{19} and 2.60×10^{19} for the measurements at 7.8 K and 202 K, respectively. The spent times are about 18.6 and 17.3 hr for the measurements at 7.8 K and 202 K, respectively. The right vertical keys show the INS intensity in arbitrary units. The intensity is normalized to compare two data in different proton numbers.

each line. We were unable to estimate accurately the energy resolution around 10 meV and 18 meV because of powder samples. The energy resolution around 10 meV and 18 meV is expected to be higher than that at 0 meV. Therefore, we compared the width of the peak with the energy resolution at 0 meV (horizontal bar). The width of the 10 meV peak in YCrGeO$_5$ is broader than the energy resolution. The 18 meV peak in ^{154}SmCrGeO$_5$ is nearly resolution

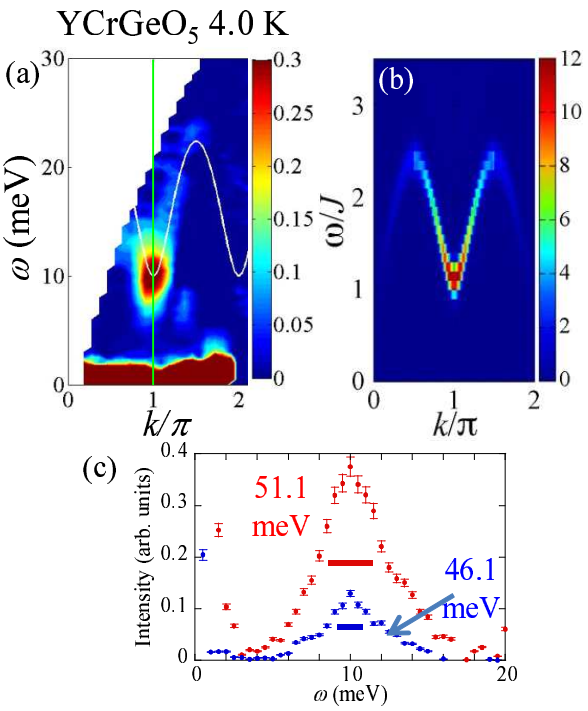

FIG. 7: (Color online) (a) Map of neutron scattering intensity in the $k-\omega$ plane of $YCrGeO_5$ at 4.0 K and $E_i = 51.1$ meV obtained using the conversion method.[31] The horizontal axis indicates the normalized wavenumber parallel to the spin chain. The right vertical key shows the INS intensity in arbitrary units. The white line indicates $\omega(k) = \sqrt{A^2 \sin^2 k + \Delta^2}$ with $\Delta = 10$ meV and $A = 20$ meV. (b) The dynamical structure factor of the AF Heisenberg alternating spin-3/2 chain with $\delta = 0.75$ calculated using the dynamical DMRG method. The right vertical key shows the intensity in arbitrary units. We used a Lorentzian broadening with half width at half maximum $\eta = 0.16J$. (c) Experimental constant-Q spectra at $k = \pi$ indicated by the green line in (a). Red and blue circles represent data at $E_i = 51.1$ and 46.1 meV (with a higher energy resolution), respectively. The horizontal bars represent the energy resolution at $\omega = 0$ meV.

limited or might be slightly broader than the energy resolution. This result is consistent with the fact that the spin system of Cr^{3+} spins in $SmCrGeO_5$ $[(1-\delta)/(1+\delta) = 0.05]$ is similar to an isolated AF dimer.

We show in Fig 3 that the experimental susceptibility is similar to the calculated one. The experimental χ_{exp} of $YCrGeO_5$ consists of three terms χ_{Cr}, χ_{CW}, and χ_0. The first term χ_{Cr} is susceptibility of the alternating spin chain with $J = 106$ K and $\delta = 0.75$. The

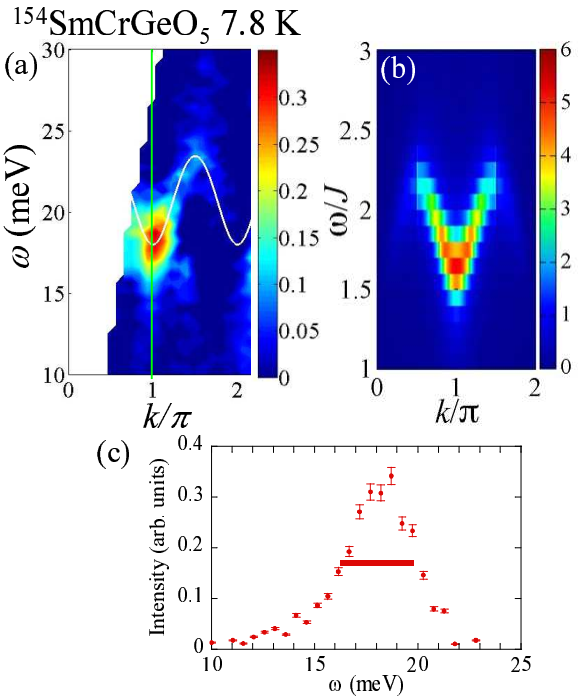

FIG. 8: (Color online) (a) Map of neutron scattering intensity in the $k-\omega$ plane of $^{154}SmCrGeO_5$ at 7.8 K and $E_i = 91.6$ meV obtained using the conversion method.[31] The horizontal axis indicates the normalized wavenumber parallel to the spin chain. The right vertical key shows the INS intensity in arbitrary units. The white line indicates $\omega(k) = \sqrt{A^2 \sin^2 k + \Delta^2}$ with $\Delta = 18$ meV and $A = 15$ meV. (b) The dynamical structure factor of the AF Heisenberg alternating spin-3/2 chain with $\delta = 0.9$ calculated using the dynamical DMRG method. The right vertical key shows the intensity in arbitrary units. We used a Lorentzian broadening with half width at half maximum $\eta = 0.16J$. (c) Experimental constant-Q spectrum (circles) at $k = \pi$ indicated by the green line in (a). The horizontal bar represents the energy resolution at $\omega = 0$ meV.

second term χ_{CW} is the Curie-Weiss term that is dominant at low T. In the two terms, we reasonably assume that the g-value is 2 for Cr^{3+} spins. From the data below 10 K, we obtained $\chi_{CW} = \frac{0.052}{T-0.2}$ emu/mol, which means that about 2.8 % of Cr spins are nearly isolated. Therefore, the green line of χ_{Cr} represents 0.972 of the molar susceptibility of the alternating spin chain. The third term χ_0 is a constant term. When $\chi_0 = -1.3 \times 10^{-4}$ emu/mol, the sum of the three terms χ_{cal} reproduces roughly the experimental χ_{exp}. We speculate that the negative value of χ_0 originates mainly in non-magnetic $Y_2Ge_2O_7$. The

sample used in the susceptibility measurement (2.8 % isolated spins) differs from that used in the high-field magnetization measurement (5 % isolated spins as aforementioned). We obtained a value close to 5 % from susceptibility of a sample took from the same batch used in the high-field magnetization measurement.

The experimental $\chi_{\rm exp}$ of $SmCrGeO_5$ consists of three terms $\chi_{\rm Cr}$, $\chi_{\rm Sm}$, and χ_0. The first term $\chi_{\rm Cr}$ is susceptibility of the alternating spin chain with $J = 128$ K and $\delta = 0.9$. The second term $\chi_{\rm Sm}$ is the Curie-Weiss term generated by Sm^{3+} ions. From the data below 30 K, we obtained $\chi_{\rm Sm} = \frac{0.055}{T+0.22}$ emu/mol. The ground state of Sm^{3+} ions is ${}^6H_{5/2}$, meaning that the value of $\boldsymbol{J}$ $(= \boldsymbol{L} + \boldsymbol{S})$ is $|L - S| = 5/2$. Here, $\boldsymbol{L}$ is the total angular momentum. The value of the Landé g factor is 2/7. Thus, the Curie constant of Sm^{3+} ions is calculated as 0.0893 emu K/mol, which is slightly larger than the experimental value. The third term χ_0 is a constant term. When $\chi_0 = 1.6 \times 10^{-3}$ emu/mol, the sum of the three terms $\chi_{\rm cal}$ reproduces roughly the experimental $\chi_{\rm exp}$.

Our INS and susceptibility results indicate that the dominant $J(1+\delta)(\equiv J_1)$ interaction is AF. In $SmCrGeO_5$, the other $J(1-\delta)(\equiv J_2)$ interaction (12.8 K) is much smaller than the J_1 interaction (243 K), indicating that the spin system is regarded as weakly-coupled AF dimers. Therefore, even if the J_2 interaction is ferromagnetic (F), our conclusion is intrinsically unchanged. In $YCrGeO_5$, we infer that the J_2 interaction must be AF. As described, the alternating spin chain with $J_1 = 186$ K and $J_2 = 26.5$ K can explain our INS and susceptibility results. In addition, the Cr-O-Cr angles suggest that the J_2 interaction in $YCrGeO_5$ is AF as follows. An exchange interaction value is determined mainly by the Cr-O-Cr angle. The angle in the d_1 bond is larger than that in the d_2 bond. Therefore, the J_1 interaction exists in the d_1 bond. The angles in the d_1 bond are 95.9° and 97.3° for $YCrGeO_5$ ($J_1 = 186$ K) and $SmCrGeO_5$ ($J_1 = 243$ K), respectively. The smaller angle is consistent with the smaller J_1 value. The angle in the d_2 bond is larger in $YCrGeO_5$ (92.8°) than $SmCrGeO_5$ (91.3°). If the J_2 interaction in $YCrGeO_5$ is F, then the J_2 interaction in $SmCrGeO_5$ is also F and the magnitude $|J_2|$ must be larger in $SmCrGeO_5$ than in $YCrGeO_5$, which is inconsistent with the INS results (stronger dispersion in $YCrGeO_5$). Consequently, it is natural to infer that the J_2 interaction in $YCrGeO_5$ is AF.

IV. CONCLUSION

We conducted inelastic neutron scattering (INS) and magnetization measurements on RCrGeO$_5$ (R = Y or Sm) powders. The high-field magnetization of YCrGeO$_5$ suggests the existence of a spin gap. We observed spin gap (singlet-triplet) excitations and the dispersion relation of the lowest magnetic excitations in the INS results. The experimental results are consistent with the calculated results of the antiferromagnetic alternating spin-3/2 chain. YCrGeO$_5$ and SmCrGeO$_5$ are the first spin-3/2 chain substances having a spin-singlet ground state with a spin gap. From the alternation ratio, the ground state is expected to be the $(2S, 0)$ state as shown in Fig. 1. We will study other RCrGeO$_5$. We expect to find substances of which ground state is the $(2S-1, 1)$ state as shown in Fig. 1.

Acknowledgments

The neutron scattering experiments on ^{154}SmCrGeO$_5$ were approved by the Neutron Scattering Program Advisory Committee of IMSS, KEK (Proposal No. 2013S01). The neutron scattering experiments on YCrGeO$_5$ were approved by the Neutron Science Proposal Review Committee of J-PARC/MLF (Proposal No. 2012B0009) and supported by the Inter-University Research Program on Neutron Scattering of IMSS, KEK. The high-field magnetization experiments were conducted under the Visiting Researcher's Program of the Institute for Solid State Physics, the University of Tokyo. This work was supported by grants from NIMS. We are grateful to S. Matsumoto for sample syntheses and X-ray diffraction measurements, to M. Kaise for X-ray diffraction measurements, and to H. Sakurai for fruitful discussion. M.K. thanks S. Yamada and S. Nishimoto for helpful discussions on numerical techniques of the DMRG method. The theoretical work was supported by KAKENHI (No. 23540428) and the World Premier International Research Center Initiative (WPI), MEXT, Japan.

[1] Y. Kato and A. Tanaka, J. Phys. Soc. Jpn. **63**, 1277 (1994).

[2] M. Kohno, M. Takahashi, and M. Hagiwara, Phys. Rev. B **57**, 1046 (1998).

[3] M. Yajima and M. Takahashi, J. Phys. Soc. Jpn. **65**, 39 (1996).

[4] S. Yamamoto, Phys. Rev. B **55**, 3603 (1997).

[5] K. M. Diederix, H. W. J. Blöte, J. P. Groen, T. O. Klaassen, and N. J. Poulis, Phys. Rev. B **19**, 420 (1979).

[6] J. C. Bonner, S. A. Friedberg, H. Kobayashi, D. L. Meier, and H. W. J. Blöte, Phys. Rev. B **27**, 248 (1983).

[7] J. W. Bray, H. R. Hart, Jr., L. V. Interrante, I. S. Jacobs, J. S. Kasper, G. D. Watkins, S. H. Wee, and J. C. Bonner, Phys. Rev. Let. **35**, 744 (1975).

[8] I. S. Jacobs, J. W. Bray, H. R. Hart, Jr., L. V. Interrante, J. S. Kasper, and G. D. Watkins, D. E. Prober, and J. C. Bonner, Phys. Rev. B **14**, 3036 (1976).

[9] M. Hase, I. Terasaki, and K. Uchinokura, Phys. Rev. Lett. **70**, 3651 (1993).

[10] M. Hase, I. Terasaki, Y. Sasago, K. Uchinokura, and H. Obara, Phys. Rev. Lett. **71**, 4059 (1993).

[11] M. Hase, I. Terasaki, K. Uchinokura, M. Tokunaga, N. Miura, and H. Obara, Phys. Rev. B **48**, 9616 (1993).

[12] Y. Narumi, M. Hagiwara, M. Kohno, and K. Kindo, Phys. Rev. Let. **86**, 324 (2001).

[13] A. Zheludev, T. Masuda, B. Sales, D. Mandrus, T. Papenbrock, T. Barnes, and S. Park, Phys. Rev. B **69**, 144417 (2004).

[14] J. P. Renard, M. Verdaguer, L. P. Regnault, W. A. C. Erkelens, J. Rossat-Mignod, and W. G. Stirling, Europhys. Lett. **3**, 945 (1987).

[15] J. Darriet and L. P. Regnault, Solid State Commun. **86**, 409 (1993).

[16] J. F. DiTusa, S-W. Cheong, C. Broholm, G. Aeppli, L. W. Rupp, Jr., and B. Batlogg, Physica B **194-196**, 181 (1994).

[17] T. Yokoo, T. Sakaguchi, K. Kakurai, and J. Akimitsu, J. Phys. Soc. Jpn. **64**, 3651 (1995).

[18] G. E. Granroth, M. W. Meisel, M. Chaparala, Th. Jolicoeur, B. H. Ward, and D. R. Talham, Phys. Rev. Let. **77**, 1616 (1996).

[19] M. Hagiwara, Y. Idutsu, Z. Honda, and S. Yamamoto, J. Phys.: Conf. Ser. **400**, 032014

(2012).

[20] G. E. Granroth, S. E. Nagler, R. Coldea, R. S. Eccleston, B. H. Ward, D. R. Talham, and M. W. Meisel, App. Phys. A **74**, S868 (2002).

[21] K. Kakurai, M. Steiner, R. Pynn, and J. K. Kjems, J. Phys.: Condens. Matter **3**, 715 (1991).

[22] S. Itoh, T. Yokoo, S. Yano, D. Kawana, H. Tanaka, and Y. Endoh, J. Phys. Soc. Jpn. **81**, 084706 (2012).

[23] S. Itoh, Y. Endoh, K. Kakurai, H. Tanaka, S. M. Bennington, T. G. Perring, K. Ohoyama, M. J. Harris, K. Nakajima, and C. D. Frost, Phys. Rev. B **59**, 14406 (1999).

[24] S. Itoh, H. Tanaka, and M. J. Bull, J. Phys. Soc. Jpn. **71**, 1148 (2002).

[25] R. V. Shpanchenko, A. A. Tsirlin, E. S. Kondakova, E. V. Antipov, C. Bougerol, J. Hadermann, G. van Tendeloo, H. Sakurai, and E. Takayama-Muromachi, J. Solid State Chem. **181**, 2433 (2008).

[26] S. Itoh, T. Yokoo, S. Satoh, S. Yano, D. Kawana, J. Suzuki, and T. J. Sato, Nucl. Instr. Meth. Phys. Research A **631**, 90 (2011).

[27] S. Yano, S. Itoh, T.Yokoo, S. Satoh, T. Yokoo, D. Kawana, and T. J. Sato, Nucl. Instr. Meth. Phys. Research A **654**, 421 (2011).

[28] S. Itoh, K. Ueno, and T. Yokoo, Nucl. Instr. Meth. Phys. Research A **661**, 58 (2012).

[29] H. G. Evertz, Adv. Phys. **52**, 1 (2003).

[30] E. Jeckelmann, Phys. Rev. B **66** 045114 (2002).

[31] K. Tomiyasu, M. Fujita, A. I. Kolesnikov, R. I. Bewley, M. J. Bull, and S. M. Bennington, Appl. Phys. Lett. **94**, 092502 (2009).